### Title

Rhesus monkeys and baboons develop clotting factor VIII inhibitors in response to porcine endothelial cells or islets




### Journal

Xenotransplantation, 21(4)

### ISSN

0908-665X



### Authors

Stewart, John M
Tarantal, Alice F
Hawthorne, Wayne J
et al.



### Publication Date

2014-07-01

### DOI

10.1111/xen.12100

Peer reviewed

Published in final edited form as:
*Xenotransplantation*. 2014 July ; 21(4): 341–352. doi:10.1111/xen.12100.

# Rhesus monkeys and baboons develop FVIII inhibitors in response to porcine endothelial cells or islets

**JM Stewart**[1], **AF Tarantal**[2], **WJ Hawthorne**[3,4], **EJ Salvaris**[5], **PJ O'Connell**[3,4], **MB Nottle**[6], **AJF d'Apice**[5,7], **PJ Cowan**[5,7], and **M Kearns-Jonker**[1]

[1]Division of Human Anatomy, Loma Linda University School of Medicine, Loma Linda, CA, USA

[2]Departments of Pediatrics and Cell Biology and Human Anatomy, and California National Primate Research Center, University of California, Davis, CA, USA

[3]Centre for Transplant and Renal Research, Westmead Millennium Institute, Westmead, NSW, Australia

[4]National Pancreas Transplant Unit, University of Sydney at Westmead Hospital, NSW, Australia

[5]Immunology Research Centre, St. Vincent's Hospital Melbourne, Victoria, Australia

[6]Discipline of Obstetrics and Gynaecology, University of Adelaide, South Australia, Australia

[7]Department of Medicine, University of Melbourne, Victoria, Australia

## Abstract

**Background—**Xenotransplantation of porcine organs holds promise of solving the human organ donor shortage. The use of α-1,3-galactosyltransferase knockout (GTKO) pig donors mitigates hyperacute rejection, while delayed rejection is currently precipitated by potent immune and hemostatic complications. Previous analysis by our laboratory suggests FVIII inhibitors might be elicited by the structurally restricted xenoantibody response which occurs after transplantation of either pig GTKO/hCD55/hCD59/hHT transgenic neonatal islet cell clusters or GTKO endothelial cells.

**Methods—**A recombinant xenoantibody was generated using sequences from baboons demonstrating an active xenoantibody response at day 28 after GTKO/hCD55/hCD59/hHT transgenic pig neonatal islet cell cluster transplantation. Rhesus monkeys were immunized with GTKO pig endothelial cells to stimulate an anti-nonGal xenoantibody response. Serum was collected at day 0 and 7 after immunization. A two stage chromogenic assay was used to measure FVIII cofactor activity and identify antibodies which inhibit FVIII function. Molecular modeling and molecular dynamics simulations were used to predict antibody structure and the residues which contribute to antibody-FVIII interactions. Competition ELISA was used to verify predictions at the domain structural level.

**Results—**Antibodies which inhibit recombinant human FVIII function are elicited after non-human primates are transplanted with either GTKO pig neonatal islet cell clusters or endothelial

Correspondence: Mary Kearns-Jonker, Loma Linda University/Division of Human Anatomy, 24760 Stewart St Ste 2215, Loma Linda, CA 92350, Tel +1 909 558 8694, mkearnsjonker@llu.edu.

cells. There is an apparent increase of inhibitor titer by 15 Bethesda units after transplant; where an increase greater than 5 Bu can indicate pathology in humans. Furthermore, competition ELISA verifies the computer modeled prediction that the recombinant xenoantibody, H66K12, binds the C1 domain of FVIII.

**Conclusions—**The development of FVIII inhibitors is a novel illustration of the potential impact the humoral immune response can have on coagulative dysfunction in xenotransplantation. However, the contribution of these antibodies to rejection pathology requires further evaluation because “normal” coagulation parameters after successful xenotransplantation are not fully understood.

### Keywords

Xenoantibody; FVIII; FVIII inhibitor; Porcine; Non-Human Primate

## Introduction

Delayed xenograft rejection of genetically modified porcine organs is a complicated process characterized by vascular antibody deposition, complement activation, hemostatic dysregulation, and potent innate and adaptive immune responses (1–4). It is currently unknown whether coagulative dysfunction is, at least in part, dependent on the antigraft immune response. The specific importance of the humoral immune system in delayed xenograft rejection is illustrated by the prolongation of median graft survival by 63 days with the addition of B cell depleting (anti-CD20) therapy in baboons transplanted with hearts from genetically modified pigs (5). Further reducing the immunogenicity of porcine grafts or selectively inhibiting xenotransplant reactive antibodies, also known as xenoantibodies, should prolong xenograft survival while preserving remaining humoral immune surveillance. Unfortunately, the identity of the antigen(s) relevant to rejection of α-1,3-galactosyltransferase knockout (GTKO) porcine organs is still an issue of debate (6–8).

Clotting factor VIII (FVIII) is a feasible non-Gal-α-1,3-Gal (nonGal) antigen given the recent discovery that endothelial cells synthesize and release FVIII not only in hepatic but also pulmonary, cardiac, intestinal, and dermal microvascular beds (9, 10). Generation of FVIII inhibitors has long been known to be a common side effect for patients with hemophilia A receiving FVIII replacement therapy (11) and have even, on occasion, been traced to the mutation of a single amino acid of FVIII (12, 13). There is only 76–90% amino acid homology between porcine and human FVIII for those domains commonly inhibited (14). The development of inhibitory anti-FVIII antibodies in a xenotransplantation setting is therefore plausible.

Our laboratory has identified and characterized the immunoglobulin germline genes that encode anti-GTKO xenoantibodies in multiple settings (15, 16). The induced immunoglobulin heavy chain variable (IGVH) genes, VH3-21 and VH3-66, are 92% similar and were in germline formation. Antibodies utilizing both these IGVH genes in germline configuration have been identified to inhibit clotting factor VIII (FVIII) in humans (17). In this report, we use a two-step chromogenic assay to identify xenoantibody FVIII inhibitors

developed in response to GTKO/hCD55/hCD59/hHT transgenic porcine neonatal islet cell cluster (NICC) transplantation in immune suppressed baboons as well as in non-immunosuppressed rhesus monkeys immunized with GTKO endothelial cells. Furthermore, we use a combination of homology modeling, *in silico* epitope prediction, competitive ELISA, and *in silico* polyalanine scanning to explore FVIII-xenoantibody interactions. The goal of our study is to characterize xenoantibody structure and xenoantibody-antigen interactions that may participate in antibody-mediated injury after xenotransplantation of genetically modified porcine organs so that this information can be used to rationally design selective immunosuppressive interventions directed at mitigating humoral rejection.

## Materials and Methods

### Construction of an Anti- NonGal Single Chain Xenoantibody

Representative cloned IgM cDNA sequences, previously isolated from baboons demonstrating an active xenoantibody response at day 28 after transplantation with GTKO/hCD55/hCD59/hHT porcine NICC xenografts (16), most closely related to the human heavy and light chain variable genes, IGVH3-66 and IGKV1D-12, were inserted into a pHEN2 phagemid [Center for Protein Engineering, Medical Research Council Center (MRC) Cambridge, UK] (18). These baboons had developed a xenoantibody response despite treatment with a typical immunosuppressive protocol; including a combination of induction with ATG and ongoing treatment with mycophenolate mofetil and tacrolimus. This single chain variable fragment (scFv) construct was named H66K12. The primers used to clone the IGVH gene were LD3 and VH3BackSFI for the first reaction and JH4XHOI and VH3BackSFI for the second reaction. The light chain primers were ApaL1.K1D12 and IGJK12NotI. All reactions included 30 cycles; each cycle was 94°C for 30 seconds, 51°C for 30 seconds, and 72°C for 1 minute. The construct was inserted in frame as determined by sequencing (Beckman Research Institute at the City of Hope, Duarte, CA) using pHEN-SEQ and For_LinkSeq primers. Primer sequences were as follows: LD3 5′ TCT GGG GGA GGC TTG GTC 3′; VH3BackSFI 5′ GTC CTC GCA ACT GCG GCC CAG CCG GCC ATG GCC CAG GTG CAG CTG GTT GAG TCT GGT CG 3′; JH4XHOI 5′ TCG ACC TCG AGC TGA GGA GAC GGT GAC CAG GAC TCC CTG GCC CCA GTA GTC CAC CAC TAT AGT AAA AAC ACC CCC TCT CGC 3′; ApaL1.K1D12 5′ GTC CTC GCA ACT GCG TGC ACA GGA CAT CCA GAT GAC CCA GTC TCC ATC TTC CGT GTC TGC ATC TGT AGG AGA CAA AGT C 3′; IGJK12NotI 5′ TCG ACG CGG CCG CTT TGA TCT CCA CTT TGG TCC CCT GGC CAA AAC TGT ACG GGT AAC TAC TAC CCT GTC GAC AGT AAT AA 3′; pHEN-SEQ 5′ CTA TGC GGC CCC ATT CA 3′; FOR_LinkSeq 5′ GCC TTT TCT GTA TGA GG 3′

### Expression and Purification of Single Chain Antibody

Chemically competent *E. coli* strain HB2151 were transfected with the single chain pHEN2 DNA construct. A 1:100 dilution of a bacterial overnight growth was used to seed 2xTY media (1% glucose, 1% Ampicillin). Bacteria were grown, shaking, at 37°C and 225 rpm until an optical density of 0.8–0.9 at 600 nm. Isopropyl β-D-1-thiogalactopyranoside was added to a final concentration of 1 mM. After 20–24 hours shaking at 225 rpm and 30°C, bacteria were cleared by centrifugation at 1,800 g at 4°C.

Protein in the bacterial supernatant was concentrated by ammonium sulfate precipitation at 80% saturation (4°C). Precipitated protein was pelleted by centrifugation for 15 minutes at 10,000 g and 4°C and resuspended to 1/50 initial volume in cold phosphate buffered saline (PBS; pH 7.4). Concentrated protein was dialyzed at 4°C to remove remaining ammonium sulfate. Protein was purified using Ni-NTA agarose resin according to manufacturer instructions, with the exception of using 10 mM imidazole wash buffer (Qiagen, Carlsbad, CA). Flow through, washes, and elutions were saved for analysis by sodium dodecyl sulfate polyacrylamide gel electrophoresis and visualized. The band at 28 KDa was quantified using Imperial Protein Stain (Thermoscientific, Rockford, IL) and carbonic anhydrase (Sigma, St. Louis, MO) standards. Total protein in Ni-NTA purified scFv preparations was determined by micro BCA assay (Thermoscientific, Rockford, IL).

### Animals

Four juvenile rhesus macaques (*Macaca mulatta*) from the California National Primate Research Center, University of California, Davis, CA were housed in accordance with The American Association for Accreditation of Laboratory Animal Care standards. All procedures were in accordance with the requirements of the Animal Welfare Act, and protocols were approved prior to implementation by the University of California, Davis Institutional Animal Care and Use Committee.

### Induction of Anti-NonGal Xenoantibodies after Immunization with Porcine GTKO Endothelial Cells

The porcine GTKO endothelial cells (PEGKO42) were kindly provided by Dr. David Sachs at Massachusetts General Hospital. Four (2.1–2.4 kg) age matched (~9 months of age) rhesus monkeys were selected for low levels of preexisting anti-nonGal xenoantibodies by ELISA using PEGKO42 as a target. Animals were immunized with $60 \times 10^6$ GTKO endothelial cells by intravenous injection (peripheral vessel). These animals were not provided any immunosuppression. Serum samples were collected at day 0 and at day 7 post-immunization.

### Flow Cytometry

The presence of anti-nonGal reactive IgM antibodies in sera was confirmed by comparison of day 0 and day 7 IgM reactivity to GTKO endothelial cells. Heat-inactivated serum samples were diluted 1/40 in sterile PBS and incubated with GTKO endothelial cells at room temperature (RT) for 60 minutes. Cells were washed with cold PBS and incubated with FITC-conjugated goat (Fab') anti-human IgM (1/50) (Jackson Immunoresearch, West Grove, PA). Cells were then washed, resuspended in cold PBS, and analyzed using a MACSQuant flow cytometer (Becton Dickinson, San Diego, CA) and FlowJo software (Tree stars, Ashland, OR). Incubation with the secondary antibody alone was used to measure background.

### Detection of FVIII inhibitors

Inhibition of FVIII cofactor activity by xenoantibodies was determined using a Technochrom two stage chromogenic assay for FVIII activity (Diapharma Group, Inc., West

Chester, OH). In this assay, the amount of FXa generated from FX is dependent on the FVIII cofactor activity of the sample of interest. Thus, FVIII activity is actually calculated from the absorbance of a chromophore produced by cleavage of a chromogen by FXa. Advate, recombinant human, von Willebrand factor (vWF) free, FVIII (Baxter Healthcare Corporation, Westlake Village, CA) was used in place of plasma-derived FVIII. FVIII was mixed with recombinant antibody/control, or serum as indicated (in the results) in the provided FVIII dilution buffer. Prepared solutions were treated as plasma samples and the remainder of the assay was performed according to the manufacturer's instructions using a microtiter plate scheme and the endpoint determination method. As indicated, readings of blank wells were used as no measurable FVIII activity. All experiments utilized a minimum of two technical replicates.

### Computational Modeling

All *in silico* work was performed using the Discovery Studio 3.5 suite (Accelrys, San Diego, CA) optimized for structural analysis of protein. All crystal structures were extracted from the Protein Data Base (RCSB.org) and are listed with their PDB ID number.

### Homology Modeling

Homology modeling makes use of amino acid sequence similarity to deposited crystal structures in order to generate a three dimensional protein model which serves as the basis for further refinements. Representative amino acid sequences were derived from cloned heavy and light chain cDNA sequences of IgM xenoantibodies induced in baboons at 28 days after transplantation of GTKO/hCD55/hCD59/hHT transgenic porcine NICC (16). The variable fragment (Fv) model of H66K12 was prepared by homology modeling using a Modeller algorithm optimized for antibody modeling. The antibody framework and complementary determining regions (CDRs) were modeled independently. Framework modeling utilized one template so as to optimize the relative positions of each chain. A combination of three crystal structures were used to model each separate CDR. Structural refinement of the heavy chain CDR3 was performed using a loop refinement protocol and the lowest energy model from the best scoring cluster was chosen for refinement using an implicit solvent-based molecular dynamics simulation in CHARM.

### *In Silico* Epitope Prediction

A computer based protocol for predicting the epitope bound by anti-FVIII antibody was first validated by accurately predicting the inhibitory FVIII epitope of Bo2C11 (1iqd) using the crystal structure of human FVIII (PDB ID 3CDZ). Epitope prediction utilized the shape based ZDOCK fast fourier docking protocol. ZRANK was used to evaluate docking results. The top ranked binding orientations (poses) from the twenty largest pose clusters were further refined using the RDOCK algorithm which incorporates electrostatic interactions. The average RMSD for the top twenty poses was calculated based on the α-carbon distances.

### Competition ELISA

The protocol for a FVIII competition ELISA was adapted from Healey et al (19). Nunc Maxisorp 96 well plates (Thermoscientific, Rockford, IL) were coated with either Ni-NTA purified recombinant single chain xenoantibody, H66K12, or protein purified from *E. coli* transfected with an empty vector matched by total protein (132 ug/ml); 50 ug/ml of recombinant scFv, H66K12, was used to coat each experimental well. Wells were coated overnight at 4°C. FVIII was diluted to 0.1 ug/ml in Hepes buffered Saline (pH 7.4) with 2 mM $CaCl_2$, 0.05% tween20, and 2% BSA. The coated plate was washed and incubated with diluted FVIII for 60 minutes at RT. Plates were washed and incubated for an hour at RT with 3 ug/ml of either GMA8010 or GMA8011 (Green Mountain Antibodies, Burlington, VA). After washing, plates were incubated with horseradish peroxidase conjugated anti-mouse IgG (1/1000) (KPL, Gaithersburg, MD) for an hour at RT. After a final wash, ABST substrate (KPL, Gaithersburg, MD) was added and allowed to develop for 15 minutes before reading. All experiments utilized a minimum of three technical replicates.

### *In Silico* Polyalanine Scanning

The most energetically favorable Fv-FVIII complex generated during epitope prediction was used to further assess the contribution of individual amino acid residues to binding. The "calculate mutation energy" protocol in Discovery Studio was used to mutate individual residues of either FVIII or the bound Fv to alanine and to determine the relative contribution of each residue to the energetics of Fv-FVIII interaction. Mutations were categorized as stabilizing or destabilizing based on the predicted change in affinity.

### Statistics

All statistical analyses were performed using Excel and data represented as mean ± standard error of the mean. Statistical significance ($p$-value $< 0.05$) compared to an untreated control was established using either a Student's t-test or ANOVA.

## Results

### The Recombinant Xenoantibody, H66K12, Inhibits FVIII Activity *In Vitro*

Our initial investigation utilized recombinant FVIII and a recombinant monoclonal scFv xenoantibody, H66K12, because of the ease with which they could be experimentally manipulated. H66K12 was constructed from representative cloned cDNA IgM sequences derived from baboons demonstrating an active xenoantibody response at day 28 after transplantation with 10,000 IEQ/Kg GTKO/hCD55/hCD59/hHT transgenic porcine NICC (Figure 1A/B). These baboons had developed a xenoantibody response despite treatment with a typical immunosuppressive protocol; including a combination of induction with ATG and ongoing treatment with mycophenolate mofetil and tacrolimus. FVIII was diluted to 150 IU/dl, 100 IU/dl, or 50 IU/dl with FVIII dilution buffer alone or in combination with either H66K12 or a control matched by total protein (50 ug/ml). The final concentration of 28 KDa xenoantibody was 7.75 ug/ml (275 nM). While this antibody concentration is well below the normal physiologic concentration of total antibody (630–1830 nM IgM + IgG), it is well above the physiologic concentration of xenoantibody (0.3–1.2 nM IgM + IgG)(20).

However, this experiment was meant to indicate, convincingly, that recombinant xenoantibody is capable of effectively inhibiting the cofactor activity of FVIII. Compared to control, H66K12 significantly inhibited FVIII cofactor activity at every concentration of FVIII ($p < 0.001$) (Figure 1C).

### Serum Derived Xenoantibody Inhibits FVIII Activity *In Vitro*

We have previously used intravenous injection of GTKO porcine endothelial cells to initiate a humoral immune response in rhesus monkeys in order to study the DNA and amino acid sequences of the induced xenoantibodies (15). These animals were not provided any form of immunosuppression. In the current study we used samples from these experiments to assay for an escalation of xenoantibodies which inhibit FVIII cofactor activity. Flow cytometry was used to measure serum IgM binding to GTKO porcine endothelial cells. At day 7, binding was 71.6% compared to 0.66% at day 0, confirming the initiation of an anti-nonGal immune response (Figure 2A).

FVIII was diluted with FVIII dilution buffer alone or in combination with either human or monkey serum (1/20 final serum dilution). FVIII concentrations were maintained within what is considered the normal human physiologic range. Inhibition of FVIII activity by pre transplant serum may reflect structural differences between human and rhesus monkey FVIII. Data collected using serum from four animals demonstrated significantly increased inhibition of FVIII cofactor activity after immunization at FVIII concentrations 150 IU/dl ($p < 0.05$), 100 IU/dl ($p < 0.05$), and 50 IU/dl ($p < 0.001$) (Figure 2B). At 150 IU/dl and 100 IU/dl FVIII concentration, activity was reduced by 60% when comparing inhibition by pre and post transplant serum. This is consistent with an increase of inhibitor titer by approximately 16 Bethesda units (Bu); where an increase over 5 Bu in humans can indicate pathology.

### Computer Modeling Predicts Induced Xenoantibody Binds the FVIII C1 Domain

Computer modeling was used to address the question of which FVIII domain was bound by H66K12. Using homology, we generated an Fv structural model. All templates used are listed in Table 1. Figure 3 depicts a Ramachandran plot demonstrating the favorable energetics of our final model. A computer based protocol for predicting the relevant epitope was first validated by accurately predicting the inhibitory FVIII epitope of Bo2C11 (1iqd) using the crystal structure of human FVIII (3CDZ). This protocol was able to accurately predict 14 of 18 FVIII residues which come within 5 A of Bo2C11 (Figure 4). The A1 domain was excluded because those FVIII inhibitors characterized to date are known to predominantly bind the A2, A3, C1, and C2 domains but not the A1 domain (19, 21). The ZDOCK docking algorithm was used to search for initial complementarity between FVIII and H66K12 based on shape. The top ranked binding orientations (poses) from the twenty largest clusters of poses were further refined using the RDOCK algorithm which incorporates electrostatic interactions. All of the top twenty final binding orientations were nearly identical (average RMSD 9.99) and bound the C1 domain. The top scoring pose bound to FVIII is illustrated in Figure 5.

### Competition ELISA Confirms Induced Xenoantibody Binds the FVIII C1 Domain

We used a competition ELISA to determine the accuracy of the *in silico* epitope prediction. We reasoned that if we captured FVIII using the recombinant xenoantibody H66K12, we should be able to detect it with an antibody which binds elsewhere on the light chain (GMA-8010) but not an inhibitory antibody which binds the C1 domain (GMA-8011). This is because H66K12 would mask the epitope recognized by GMA-8011 but not by GMA-8010. Our results illustrated in Figure 6 demonstrate that the *in silico* prediction was correct. FVIII captured by H66K12 is detectable with GMA-8011 but not by GMA-8010. Furthermore, this effect is not present if a control protein suspension generated from an empty vector is used to “capture” FVIII.

### *In Silico* Binding Site Mutation Analysis

In order to determine which residues of both H66K12 and FVIII contribute the most to binding, polyalanine scanning was performed *in silico*. Table 2 provides a list of residues which, when mutated, stabilize or destabilize the protein-protein interaction. Those residues in the xenoantibody are of particular interest. The heavy chain amino acid sequence induced in baboons in response to transplantation of GTKO/hCD55/hCD59/hHT transgenic porcine NICC and in rhesus monkeys immunized with GTKO porcine endothelial cells are 92% similar (16). Furthermore, the light chain germline variable genes utilized in response to wild type porcine organs and GTKO/hCD55/hCD59/hHT are the same (16). Here we report that the most important amino acids of both the heavy and light chains are conserved in each case; Tyr33 in the heavy chain and Trp32 in the light chain. Thus, rational design of xenoantibody inhibitors would target these residues.

Alignment of human and porcine amino acid sequences of FVIII (Figure 7A) demonstrates that most amino acid residues, which are predicted, to contribute to this interaction are conserved. Interestingly, Phe2068, present only in human FVIII, is predicted to be the most important individual amino acid. Those FVIII residues which are predicted to interact favorably with xenoantibody (the most destabilizing mutations) are illustrated in Figure 7B.

## Discussion

The impact of the immune system on coagulation dysregulation during xenotransplantation and xenograft rejection remains to be fully elucidated. We report the generation of antibodies, which inhibit human FVIII cofactor activity after transplantation of immunosuppressed baboons with GTKO/hCD55/hCD59/hHT transgenic porcine NICC and immunization of rhesus monkeys with GTKO porcine endothelial cells. While a prothrombotic response, such as consumptive coagulopathy, is predominant during acute xenograft rejection within hours to days, development of FVIII inhibitors is likely to impact long term xenotransplantation. The recombinant xenoantibody, H66K12, generated from post NICC xenotransplantation IgM xenoantibody sequences, binds to the C1 domain of FVIII. Targeting the xenoantibody pocket, which makes contact with FVIII, may be a promising strategy for selectively countering these inhibitors. However, it is unknown whether other FVIII domains are targeted as well. Nevertheless, FVIII inhibitors developed

in response to transplantation with GTKO cells represent a novel pathologic effect on recipient physiology.

FVIII is synthesized as a 330-KDa precursor protein with an A1-α1-A2-α2-B-α3-A3-C1-C2 domain structure (21). Inhibitory antibodies against FVIII are known to bind several domains including the A2, A3, C1, and C2 domains in addition to the acidic α1 region between the A1 and A2 domains. In humans, inhibitors against the C2 domain have been primarily determined to belong to the $VH_1$ family (22). However, these antibodies are often extensively modified by hypersomatic mutation and have atypically long CDR3 loops (20–23 amino acids). In contrast, inhibitors which bind the A2 and A3 domains display more variation. Anti-A2 antibodies have been reported from $VH_1$, $VH_3$, $VH_5$, and $VH_6$ families while anti-A3 antibodies are derived from $VH_1$ and $VH_3$ families (23, 24). By comparison the VH genes which generate inhibitors of the C1 domain have not been previously characterized. However, analysis of the deposited sequence of KM33, which binds the C1 residues Lys2092 and Phe2093 (25), demonstrates 87.8% identity to IgHV3-30 providing an additional C1 inhibitor which utilizes a member of the $VH_3$ family. The light chain antibodies which contribute to FVIII inhibitors have not been so extensively characterized. However, similar to H66K12, KM33 also utilizes a $VK_1$ family member, and demonstrates 86.2% identity to IgKV1-6.

FVIII inhibitors which bind the C1 domain can affect interactions with either vWF (26) or phosphatidylserine (27, 28). Given that the FVIII preparation utilized in this study is vWF factor free (29), inhibition of membrane binding is the more relevant mechanism *in vitro* for the induced xenoantibody. However, human antibodies which bind to FVIII Arg2150 inhibit FVIII binding to vWF. Since H66K12 is predicted to interact with Arg2150, it likely inhibits this interaction and would reduce FVIII half-life *in vivo*. The C1 domain is known to contribute to membrane binding (27) via Lys2092 and Phe2093 (28); however, these residues are relatively distant from the predicted binding site. Recent experiments using fluorescence energy resonance transfer have determined the angle at which FVIII interacts with phospholipid membranes (30). Given the distance from Lys2092 and Phe2093, H66K12 might bind residues which interact directly with phospholipid or act in a steric fashion. At least one amino acid predicted to interact with H66K12, Trp2046, is only one residue away from a large, positively charged region of the FVIII C1 domain predicted to interact with negatively charged phosphatidylserine. Binding of FVIII to vWF significantly increases its half-life while interaction with phospholipid is essential for cofactor function (21). *In vivo*, it is likely that both of these mechanisms can contribute to diminished FVIII function. However, the specific mechanism(s) by which induced xenoantibody inhibits FVIII function will require further investigation.

In this study, we used human FVIII as a source of primate FVIII assuming the sequences are largely similar; the sequences of rhesus monkey and baboon FVIII have not been characterized. In the context of xenotransplantation, it is reasonable to speculate that FVIII inhibitors are initiated by porcine FVIII. Humans can “break” tolerance when they develop acquired hemophilia A (31) or when provided an exogenous source of FVIII via FVIII replacement therapy (11–13). Thus, xenotransplantation may trigger a lapse in tolerance to the FVIII autoantigen by providing a source of exogenous FVIII. Four of five FVIII residues

predicted to interact most favorably with H66K12 are conserved between pigs and humans. However, a single amino acid difference can contribute to the development of inhibitors (12, 13) and humanization of porcine FVIII C1 may preempt formation of antibodies directed at this domain. Of note, there is evidence that anti-CD20 therapy can mitigate the acquisition of FVIII inhibitors in both acquired and inherited hemophilia A (31). However, in the context of xenotransplantation, anti-CD20 therapy represents a significant addition to an already cumbersome immunosuppressive burden.

The prevalence of induced anti-FVIII antibodies in other xenotransplantation settings is currently unknown. However, FVIII has recently been demonstrated to be expressed in the microvasculature of multiple sites including the liver but also lung, heart, intestine, and dermis (9, 10). Each model of xenotransplantation has variations in pathology and time to rejection with typical immunosuppressive regimens (32–37). Current reports in xenotransplantation provide clues as to where antibodies against FVIII might contribute to pathology.

The level of FVIII in the porcine serum is significantly higher than that of baboons (38). When the anti-fibrinolytic agent Amicar is provided before xenograft reperfusion to prevent thrombocytopenia, it does not overcome spontaneous bleeding. Initial investigations provide normal coagulation parameters for genetically modified pigs or typical primate species utilized in xenotransplantation (39). However, the “normal” coagulation parameters expected after xenotransplantation are currently under investigation (4, 38). Our results indicate pre transplant serum antibody can affect FVIII activity and further obscure the practicality of traditional assays using human clotting factors. In order to thoroughly dissect coagulation dysregulation in xenotransplantation, partial thromboplastin time and international normalized ratio assessment should be used in combination with ELISA for clotting factors and chromogenic assays to assess specific factor activity levels and the impact of acquired inhibitors.

Mohiuddin et al. reported extended survival times during cardiac xenotransplantation with the addition of B cell depleting therapy (5). However, the presence of remaining IgM, but primarily IgG, deposition at explant provides evidence of remaining humoral impact. Interestingly, three of those animals with extended survival times were noted to have died from abdominal bleeding due to unknown causes.

Our co-authors have recently performed thromboelastographic analysis of cynomolgus monkeys after transplantation of porcine GTKO kidneys with various transgenes. They demonstrate progressive prolongation of clotting time via the intrinsic clotting cascade which could be accounted for by either severe deficiencies of the intrinsic clotting cascade or alternatively, FVIII inhibitors (4). However, the expression of FVIII in the renal microvasculature has never been investigated.

The specific impact of anti-FVIII antibodies on delayed humoral xenograft rejection in each model of xenotransplantation will require further investigation. Whether FVIII inhibitors precipitate graft rejection or exacerbate more prevalent xenograft pathology will need to be determined. Those grafts which survive long enough to be subject to an adaptive humoral

response are more likely to generate FVIII inhibitors. Future experiments should incorporate monitoring of anti-FVIII antibodies. The development of FVIII inhibitors in xenotransplantation is, however, an illustration of the functional impact the humoral immune response can illicit. The expansion of xenoantibodies, which are capable of binding both human and nonhuman primate proteins, is not likely to be an isolated incident and xenoantibodies may have other functional effects which alter the physiology of both host and graft. Acknowledgements We thank Nancy Appleby, Yan Chen, and Tania Fuentes for technical assistance. This project was supported by NIH grant 7R01AI052079-06 to MKJ and the Primate Center base operating grant #OD011107.

## Abbreviations

| | |
|---|---|
| **nonGal** | non-Gal-α-1,3-Gal |
| **FVIII** | clotting factor VIII |
| **NICC** | neonatal islet cell cluster |
| **scFv** | single chain variable fragment |
| **vWF** | von Willebrand factor |
| **Fv** | fragmemt |
| **CDRs** | complementary determining regions |

## References

1. SHIMIZU A, YAMADA K, ROBSON SC, et al. Pathologic characteristics of transplanted kidney xenografts. J Am Soc Nephrol. 2012; 23:225–235. [PubMed: 22114174]
2. MCGREGOR CGA, RICCI D, MIYAGI N, et al. Human CD55 expression blocks hyperacute rejection and restricts complement activation in gal knockout cardiac xenografts. Transplantation. 2012; 93:686–692. [PubMed: 22391577]
3. EZZELARAB M, GARCIA B, AZIMZADEH A, et al. The innate immune response and activation of coagulation in alpha 1,3-galactosyltransferase gene-knockout xenograft recipients. Transplantation. 2009; 87:805–812. [PubMed: 19300181]
4. SPIEZIA L, BOLDRIN M, RADU C, et al. Thromboelastographic evaluation of coagulative profiles in pig-to-monkey kidney xenotransplantation. Xenotransplantation. 2013; 20:89–99. [PubMed: 23406330]
5. MOHIUDDIN MM, CORCORAN PC, SINGH AK, et al. B-cell depletion extends the survival of GTKO.hCD46Tg pig heart xenografts in baboons for up to 8 months. Am J Transplant. 2012; 12:763–771. [PubMed: 22070772]
6. CHIHARA RK, LUTZ AJ, PARIS LL, et al. Fibronectin from alpha 1,3-galactosyltransferase knockout pigs is a xenoantigen. Journal Surg Res. 2013
7. BREIMER ME. Gal/non-Gal antigens in pig tissues and human non-Gal antibodies in the GalT-KO era. Xenotransplantation. 2011; 18:215–228. [PubMed: 21848538]
8. BYRNE GW, STALBOERGER PG, DAVILA E, et al. Proteomic identification of non-Gal antibody targets after pig-to-primate cardiac xenotransplantation. Xenotransplantation. 2008; 15:268–276. [PubMed: 18957049]
9. SHAHANI T, COVENS K, LAVEND'HOMME R, et al. Human liver sinusoidal endothelial cells but not hepatocytes contain FVIII. Journal Thromb Haemost. 2013
10. SHAHANI T, LAVEND'HOMME R, LUTTUN A, et al. Activation of human endothelial cells from specific vascular beds induces the release of a FVIII storage pool. Blood. 2010; 115:4902–4909. [PubMed: 20351306]

11. EHRENFORTH S, KREUZ W, SCHARRER I, et al. Incidence of development of factor-VIII and factor -IX inhibitors in hemophiliacs. Lancet. 1992; 339:594–598. [PubMed: 1347102]
12. PEERLINCK K, JACQUEMIN MG, ARNOUT J, et al. Antifactor VIII antibody inhibiting allogeneic but not antologous factor VIII in patients with mild hemophilia A. Blood. 1999; 93:2267–2273. [PubMed: 10090936]
13. FIJNVANDRAAT K, TURENHOUT EA, VAN DEN BRINK EN, et al. The missense mutation Arg593 --> Cys is related to antibody formation in a patient with mild hemophilia A. Blood. 1997; 89:4371–4377. [PubMed: 9192760]
14. HEALEY JF, LUBIN IM, LOLLAR P. The cDNA and derived amino acid sequence of porcine factor VIII. Blood. 1996; 88:4209–4214. [PubMed: 8943856]
15. KIERNAN K, HARNDEN I, GUNTHART M, et al. The anti-non-gal xenoantibody response to xenoantigens on gal knockout pig cells is encoded by a restricted number of germline progenitors. Am J Transplant. 2008; 8:1829–1839. [PubMed: 18671678]
16. CHEN Y, STEWART JM, GUNTHART M, et al. Xenoantibody response to porcine islet cell transplantation using GTKO, CD55, CD59, and fucosyl-transferase multiple transgenic donors. Xenotransplantation. 2014 In Press.
17. GHARAGOZLOU S, KARDAR GA, RABBANI H, SHOKRI F. Molecular analysis of the heavy chain variable region genes of human hybridoma clones specific for coagulation factor VIII. Thromb Haemost. 2005; 94:1131–1137. [PubMed: 16411384]
18. KEARNS-JONKER M, SWENSSON J, GHIUZELI C, et al. The human antibody response to porcine xenoantigens is encoded by IGHV3-11 and IGHV3-74 IgVH germline progenitors. J Immunol. 1999; 163:4399–4412. [PubMed: 10510381]
19. HEALEY JF, PARKER ET, BARROW RT, et al. The humoral response to human factor VIII in hemophilia A mice. J Thromb Haemost. 2007; 5:512–519. [PubMed: 17181826]
20. KLEIHAUER A, GREGORY CR, BORIE DC, et al. Identification of the VH genes encoding xenoantibodies in non-immunosuppressed rhesus monkeys. Immunology. 2005; 116:89–102. [PubMed: 16108821]
21. LAVIGNE-LISSALDE G, ROTHSCHILD C, POUPLARD C, et al. Characteristics, mechanisms of action, and epitope mapping of anti-factor VIII antibodies. Clin Rev Allergy Immunol. 2009; 37:67–79. [PubMed: 19172415]
22. LAVIGNE-LISSALDE G, SCHVED JF, GRANIER C, VILLARD S. Anti-factor VIII antibodies: a 2005 update. Thromb Haemost. 2005; 94:760–769. [PubMed: 16270627]
23. VAN DEN BRINK EN, TURENHOUT EA, DAVIES J, et al. Human antibodies with specificity for the C2 domain of factor VIII are derived from VH1 germline genes. Blood. 2000; 95:558–563. [PubMed: 10627462]
24. VAN DEN BRINK EN, BRIL WS, TURENHOUT EA, et al. Two classes of germline genes both derived from the V(H)1 family direct the formation of human antibodies that recognize distinct antigenic sites in the C2 domain of factor VIII. Blood. 2002; 99:2828–2834. [PubMed: 11929772]
25. MERTENS, K.; BOVENSCHEN, A.; VOORBERG, J., et al. Antagonists of factor VIII interaction with low-density lipoprotein receptor-related protein. WO Patent 2,003,093,313. 2003.
26. JACQUEMIN M, BENHIDA A, PEERLINCK K, et al. A human antibody directed to the factor VIII C1 domain inhibits factor VIII cofactor activity and binding to von Willebrand factor. Blood. 2000; 95:156–163. [PubMed: 10607698]
27. HSU TC, PRATT KP, THOMPSON AR. The factor VIII C1 domain contributes to platelet binding. Blood. 2008; 111:200–208. [PubMed: 17916745]
28. MEEMS H, MEIJER AB, CULLINAN DB, et al. Factor VIII C1 domain residues Lys 2092 and Phe 2093 contribute to membrane binding and cofactor activity. Blood. 2009; 114:3938–3946. [PubMed: 19687511]
29. D'AMICI GM, TIMPERIO AM, GEVI F, et al. Recombinant clotting factor VIII concentrates: Heterogeneity and high-purity evaluation. Electrophoresis. 2010; 31:2730–2739. [PubMed: 20737444]
30. WAKABAYASHI H, FAY PJ. Molecular orientation of factor VIIIa on the phospholipid membrane surface determined by fluorescence resonance energy transfer. Biochem J. 2013; 452:293–301. [PubMed: 23521092]

31. SHETTY S, BHAVE M, GHOSH K. Acquired hemophilia A: Diagnosis, aetiology, clinical spectrum and treatment options. Autoimmun Rev. 2011; 10:311–316. [PubMed: 21115138]
32. NGUYEN BN, AZIMZADEH AM, ZHANG T, et al. Life-supporting function of genetically modified swine lungs in baboons. J Thorac Cardiovasc Surg. 2007; 133:1354–1363. [PubMed: 17467457]
33. HISASHI Y, YAMADA K, KUWAKI K, et al. Rejection of cardiac xenografts transplanted from alpha1,3-galactosyltransferase gene-knockout (GalT-KO) pigs to baboons. Am J Transplant. 2008; 8:2516–2526. [PubMed: 19032222]
34. TAZELAAR HD, BYRNE GW, MCGREGOR CGA. Comparison of gal and non-Gal-mediated cardiac xenograft rejection. Transplantation. 2011; 91:968–975. [PubMed: 21403591]
35. BUSH EL, BARBAS AS, HOLZKNECHT ZE, et al. Coagulopathy in alpha-galactosyl transferase knockout pulmonary xenotransplants. Xenotransplantation. 2011; 18:6–13. [PubMed: 21342283]
36. EKSER B, KLEIN E, HE J, et al. Genetically-engineered pig-to-baboon liver xenotransplantation: histopathology of xenografts and native organs. PloS one. 2012; 7:e29720. [PubMed: 22247784]
37. SHIMIZU A, YAMADA K, ROBSON SC, et al. Pathologic characteristics of transplanted kidney xenografts. J Am Soc Nephrol. 2012; 23:225–235. [PubMed: 22114174]
38. KIM K, SCHUETZ C, ELIAS N, et al. Up to 9-day survival and control of thrombocytopenia following alpha1,3-galactosyl transferase knockout swine liver xenotransplantation in baboons. Xenotransplantation. 2012; 19:256–264. [PubMed: 22909139]
39. EKSER B, BIANCHI J, BALL S, et al. Comparison of hematologic, biochemical, and coagulation parameters in alpha1,3-galactosyltransferase gene-knockout pigs, wild-type pigs, and four primate species. Xenotransplantation. 2012; 19:342–354. [PubMed: 23145497]

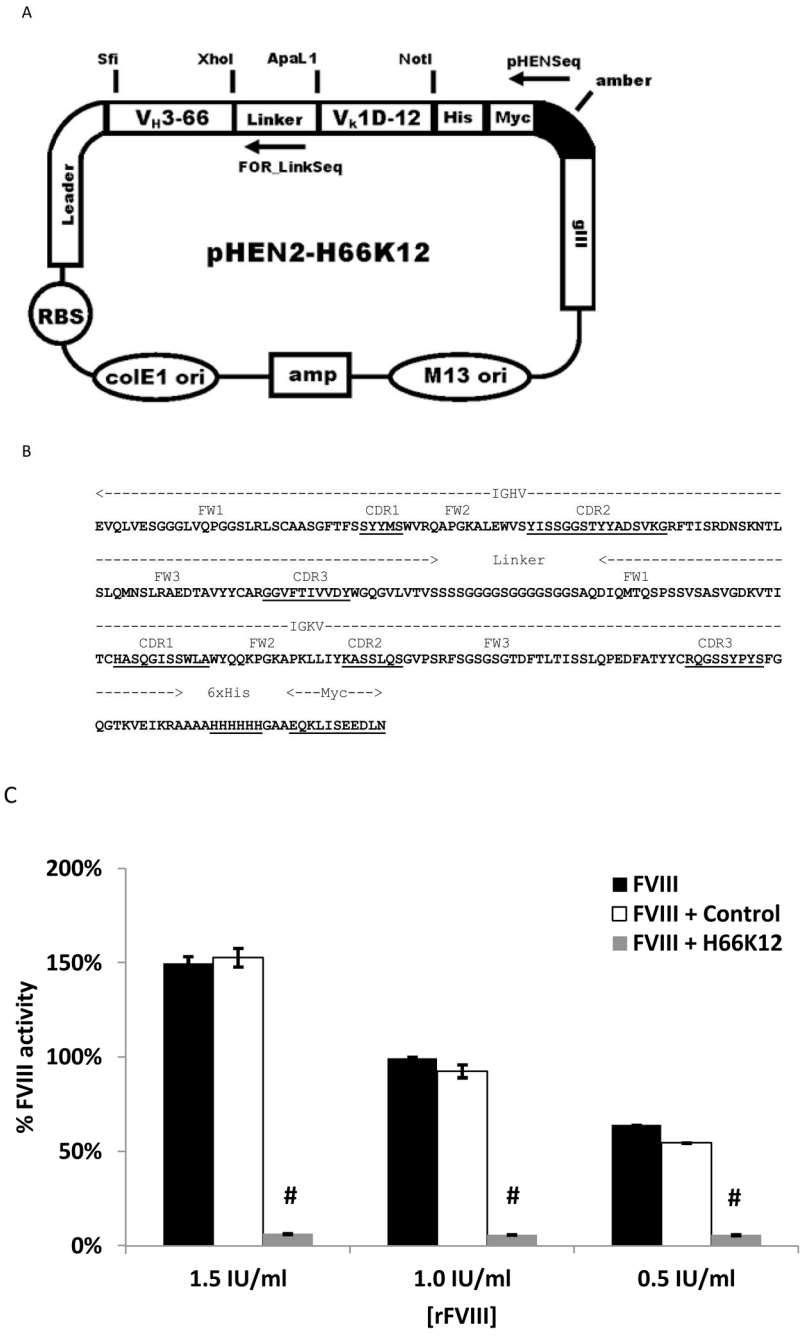


**Figure 1. Recombinant single chain xenoantibody (H66K12) inhibits FVIII cofactor activity**

A recombinant single chain xenoantibody, H66K12, was constructed from representative cloned cDNA IgM sequences derived from baboons demonstrating an active xenoantibody response at day 28 after transplantation with GTKO/hCD55/hCD59/hHT transgenic porcine NICC. **(A)** Schematic of pHEN phagemid containing the H66K12 single chain antibody encoded by the IGHV3-66 and IGKV1-12 germline genes. **(B)** Amino acid translation of the recombinant anti-nonGal single chain antibody H66K12. Complementary determining regions are labeled according to the Kabat annotation system. **(C)** Recombinant FVIII was

diluted to the final concentration indicated. FVIII alone or FVIII with 50 ug/ml of protein (control) was used for comparison. H66K12 was added to a final concentration of 7.75 ug/ml (275 nM) and matched to the control by total protein. A two-stage chromogenic assay was used to determine resulting FVIII cofactor activity. H66K12 significantly inhibited FVIII cofactor activity. (# indicates $p < 0.001$). Ampicillin resistance gene (amp), origin of replication (ori), Ribosomal binding site (RBS), Heavy chain (IGVH), Light chain (IGKV), FWR (framework region), CDR (complementarity determining region), Recombinant xenoantibody (H66K12) - rXAb.

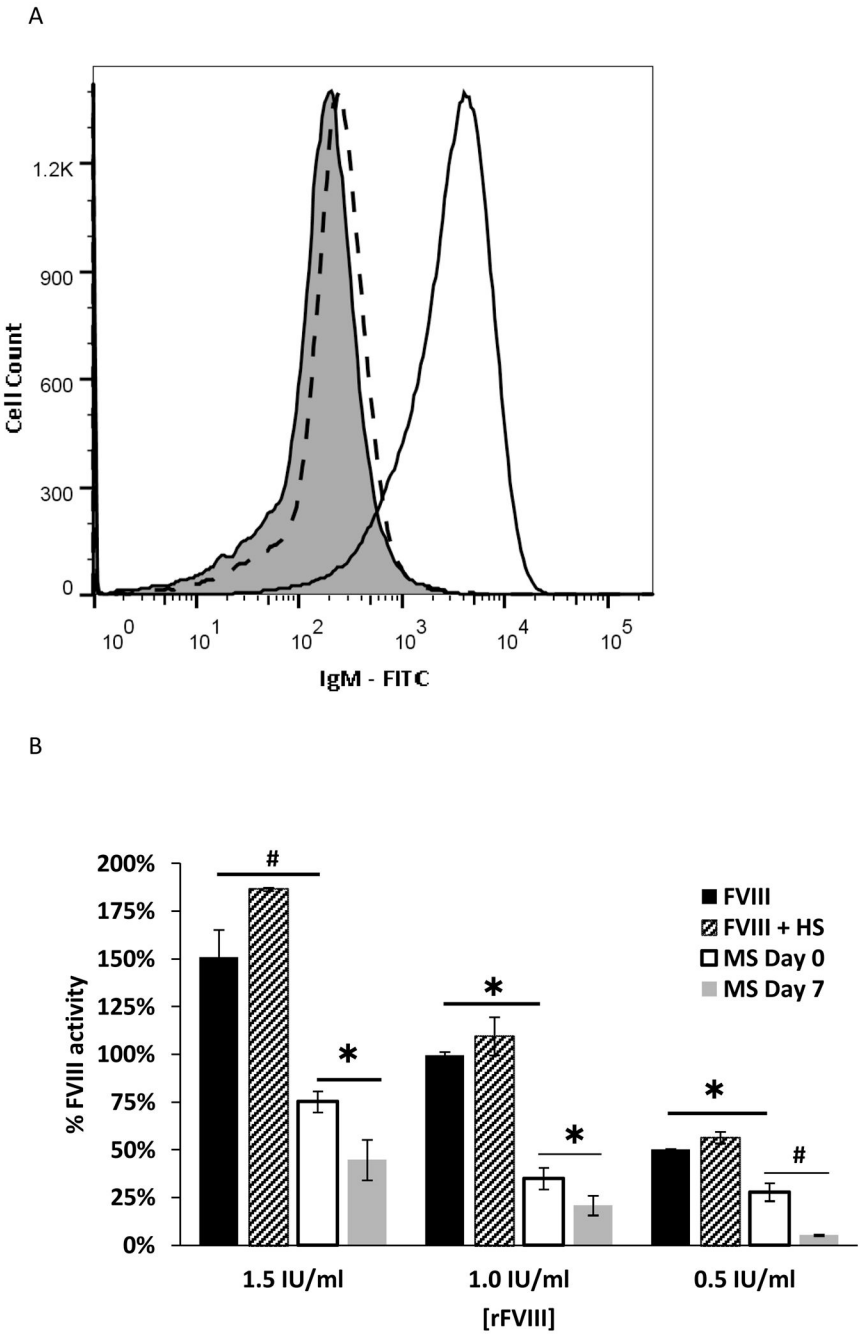


**Figure 2. Serum antibody from rhesus monkeys immunized with GTKO porcine endothelial cells inhibits FVIII cofactor activity**

(A) Rhesus monkeys were immunized with GTKO porcine endothelial cells to stimulate an anti-nonGal humoral immune response. Flow cytometry was used to measure serum IgM binding to GTKO endothelial cells. The dashed and solid curves with no shading represent binding at days 0 and 7, respectively. The shaded curve represents background determined by incubation with secondary antibody alone. (B) A two-stage chromogenic assay was used to measure FVIII activity. Recombinant FVIII was diluted to the final concentrations indicated. FVIII alone or FVIII with human serum diluted 1/20 was used as controls. The

extent to which FVIII cofactor activity was inhibited by xenoantibody at day 0 and 7 was compared in four animals. There was a significant decrease in FVIII cofactor activity with the addition of post-immunization serum at day 7, compared to day 0, at every FVIII dilution. (* indicates $p < 0.05$; # indicates $p < 0.001$) Human serum – HS; Monkey serum (MS).

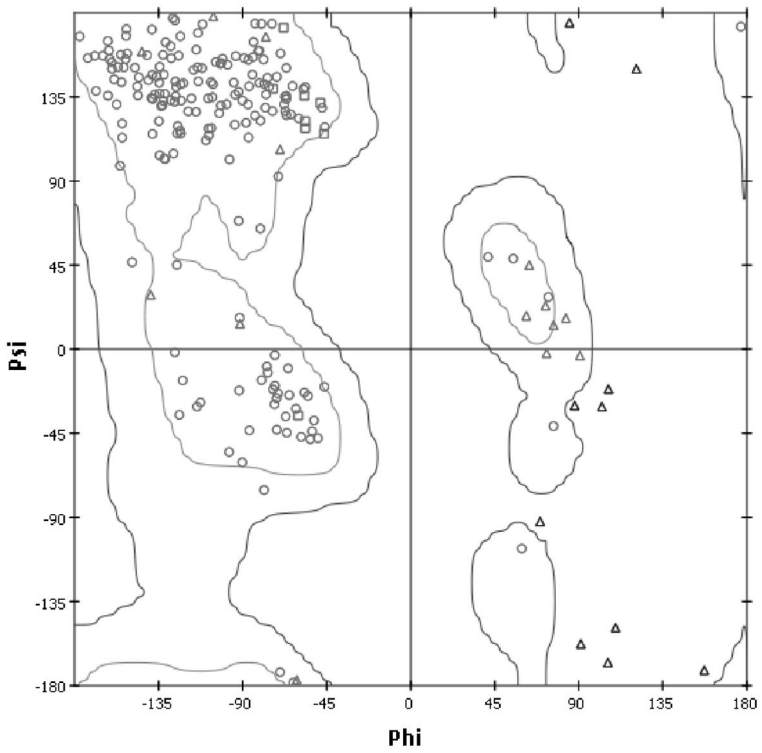


**Figure 3. Ramachandran plot of the refined model of H66K12**

Ramachandran plot of the refined model of the xenoantibody derived from representative cloned cDNA IgM sequences from baboons demonstrating an active xenoantibody response at day 28 after transplantation with GalKO/hCD55/hCD59/hHT transgenic porcine islets. Triangles represent glycine residues, squares represent proline residues, while circles represent all other amino acids.

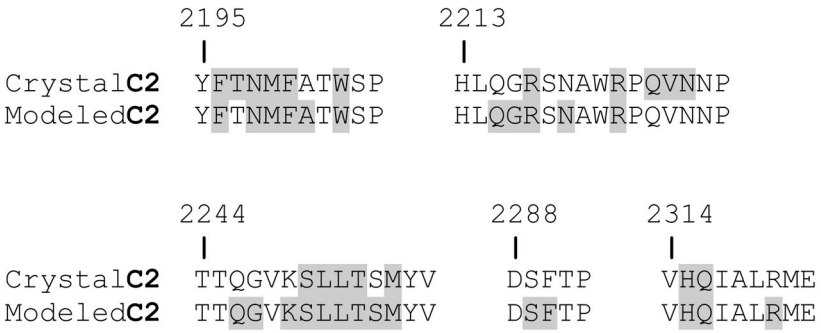


**Figure 4. Molecular modeling accurately predicts 14/18 FVIII C2 domain amino acid residues that make contact with Bo2C11**

A computer-based protocol for predicting the epitope bound by a particular anti-FVIII antibody was first validated by accurately predicting the domain bound by Bo2C11. Of 18 FVIII residues which come within 5 Å of Bo2C11 in the deposited crystal structure (PDB ID 1iqd), 14 residues are accurately predicted using molecular modeling. Highlighted residues come within 5 Å of Bo2C11; Modeled C2 indicates residues predicted using computer modeling.

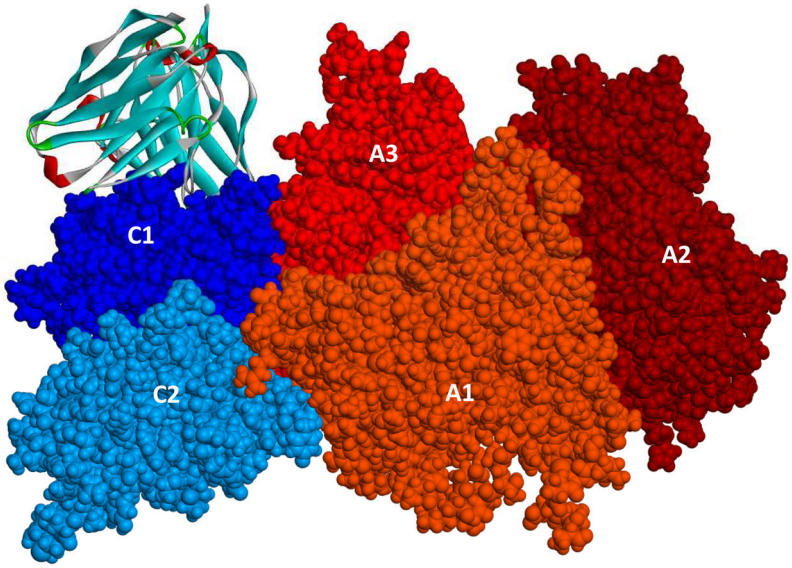


**Figure 5.** ***In silico*** **protein-docking algorithms predict xenoantibody binds the FVIII C1 domain**

Representative cloned IgM cDNA sequences from baboons actively responding to transplantation of GTKO/hCD55/hCD59/hHT porcine NICC were used to model the variable fragment of H66K12 by homology. Docking this antibody model with the crystal structure of human FVIII (PDB ID 3CDZ) using shape complementarity, then refinement with electrostatics, predicted binding to the C1 domain of FVIII. FVIII is depicted as a space filling model and domains are labeled. The best binding motif of H66K12 is depicted as a ribbon model.

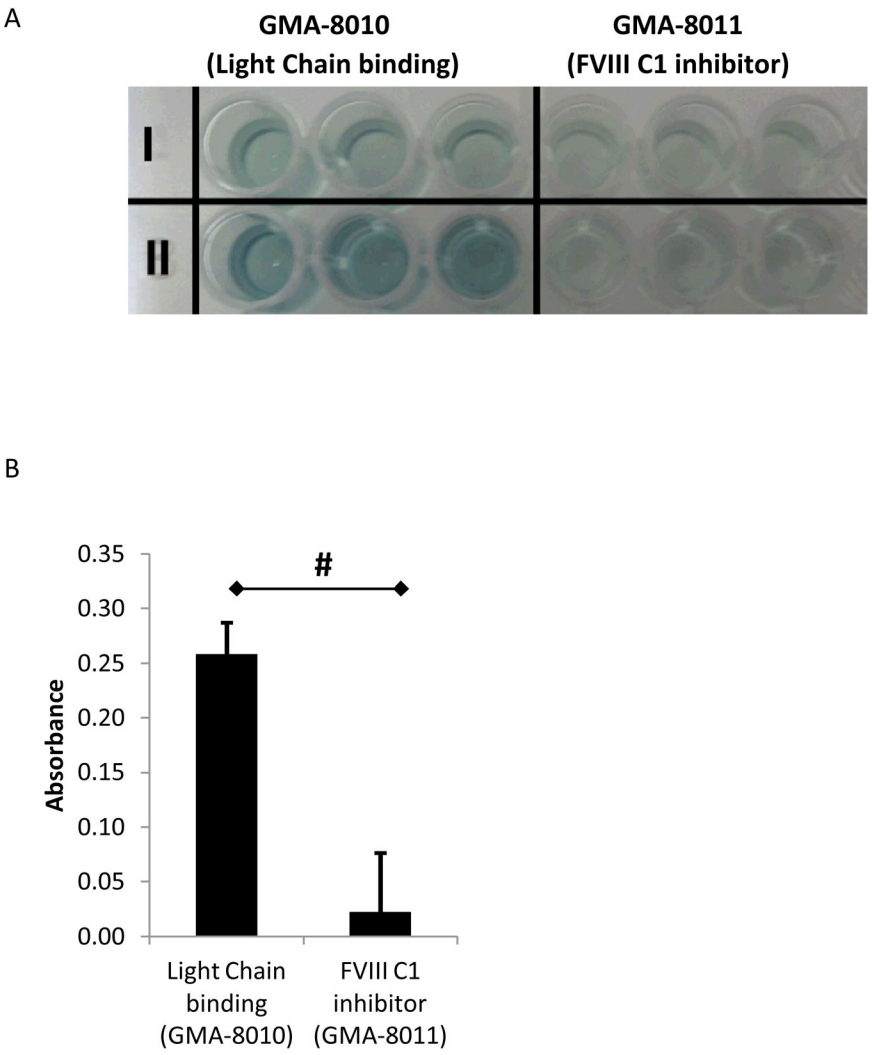


**Figure 6. Competition ELISA confirms xenoantibody binds to the FVIII C1 domain**

Protein generated from a control construct (I) or H66K12 (50 ug/ml) (II) was used to capture FVIII. Capture solutions were matched for total protein content of 132 ug/ml. FVIII was detected with either a FVIII C1 domain-binding inhibitory antibody (GMA-8011) or an antibody which binds elsewhere on the FVIII light chain (GMA-8010). The results are illustrated both as a picture (A) and as a graph (B). # indicates $p < 0.01$; Light chain – LC; A – control capture solution; B – Capture with recombinant xenoantibody.

A

```
            2010       2030       2040       2050       2060       2070
              |          |          |          |          |          |
HSFVIII-C1  KCQTPLGMASGHIRDFQITASGQYGQWAPKLARLHYSGSINAWSTKEPFSW
SSFVIII-C1  E--AP------R--------------------------------D-H--

                    2080       2090       2100       2110       2120
                      |          |          |          |          |
HSFVIII-C1  IKVDLLAPMIIHGIKTQGARQKFSSLYISQFIIMYSLDGKKWQTYRGNSTG
SSFVIII-C1  --------------M------------------------RN--S-------

                   2130       2140       2150       2160       2170
                     |          |          |          |          |
HSFVIII-C1  TLMVFFGNVDSSGIKHNIFNPPIIARYIRLHPTHYSIRSTLRMELMGCDLN
SSFVIII-C1  ----------A------------V--------------------------
```

B

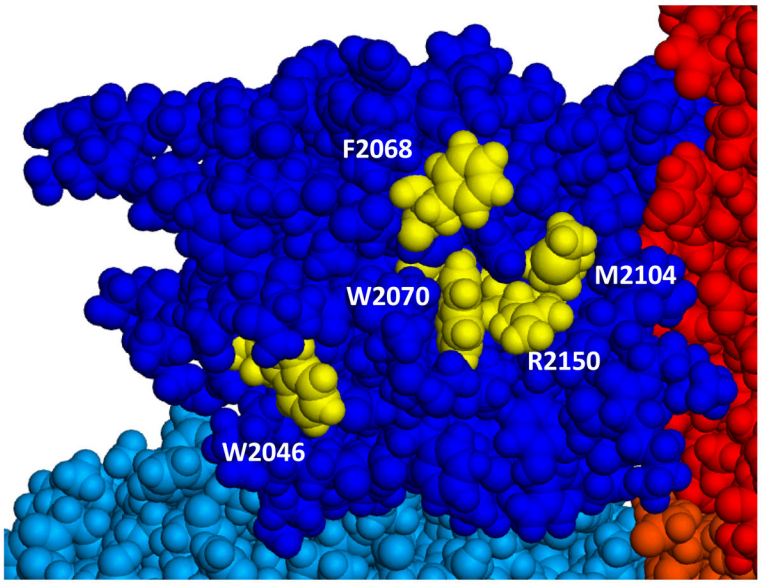


**Figure 7. Four of five FVIII residues important for xenoantibody binding are homologous with porcine FVIII**

(A) Alignment of human and porcine FVIII amino acid sequences with residues thought to contribute to binding recombinant xenoantibody highlighted and in bold. (B) The structure of FVIII C1 domain (blue) with predicted binding sites labeled and highlighted in yellow. (*Sus scrofa* accession NM_214167.1; *Homo sapiens* extracted from crystal structure PDB ID 3cdz)

**Table 1**

| Region | PDB | Similarity | Identity | Resolution | Organism |
|---|---|---|---|---|---|
| HFR | 3bn9 | 98.9% | 90.1% | 2.173 | Homo sapiens |
| LFR | 3bn9 | 94.5% | 94.4% | 2.173 | Homo sapiens |
| HCDR1 | 1fh5 | 100.0% | 100.0% | 2.9 | Homo sapiens |
| | 2h1p | 100.0% | 87.5% | 2.4 | Mus musculus |
| | 2v17 | 87.5% | 75.0% | 1.65 | Mus musculus |
| HCDR2 | 3ls5 | 85.7% | 85.7% | 1.9 | Mus musculus |
| | 3cfb | 85.7% | 85.7% | 1.6 | Mus musculus |
| | 3utz | 85.7% | 85.7% | 2.18 | Escherichia coli |
| HCDR3 | 3l95 | 66.7% | 58.3% | 2.19 | Escherichia coli |
| | 3r1g | 58.3% | 50.0% | 2.8 | Homo sapiens |
| | 3eyo | 75.0% | 41.7% | 2.5 | Homo sapiens |
| LCDR1 | 3hmw | 100.0% | 100.0% | 3 | Homo sapiens |
| | 3bn9 | 100.0% | 83.3% | 2.173 | Homo sapiens |
| | 2x7l | 83.3% | 83.3% | 3.17 | Escherichia coli |
| LCDR2 | 1dfb | 100.0% | 100.0% | 2.7 | Homo sapiens |
| | 2cmr | 100.0% | 100.0% | 2 | Homo sapiens |
| | 3ncj | 66.7% | 66.7% | 1.6 | Homo sapiens |
| LCDR3 | 1yjd | 88.9% | 55.6% | 2.7 | Mus musculus |
| | 3ncj | 77.8% | 44.4% | 1.6 | Homo sapiens |
| | 1iai | 77.8% | 55.6% | 2.9 | Mus musculus |

H- heavy; L- light; FR- framework region; CDR- complementary determining region

**Table 2**

| FVIII - C1 | Kcal/mol* | Fv - LC | Kcal/mol* | Fv - HC | Kcal/mol* |
|---|---|---|---|---|---|
| Arg2150 | +1.72 | Lys50 | −2.45 | Try100c | +1.29 |
| Met2104 | +1.82 | Ser30 | −1.92 | Tyr33 | +2.58 |
| Trp2046 | +2.07 | Ser31 | −1.84 | | |
| Trp2070 | +2.42 | Leu33 | −1.52 | | |
| Phe2068 | +4.43 | Ser53 | −1.26 | | |
| | | Ser52 | −1.22 | | |
| | | Gly91 | +1.20 | | |
| | | Try95e | +1.74 | | |
| | | Trp32 | +5.18 | | |

Fv- variable fragment; LC- light chain; HC- heavy chain;

* predicted